

LITTON SYSTEMS INC WOODLAND HILLS CA GUIDANCE AND CO--ETC F/6 7/4
NUCLEAR MOMENT ALIGNMENT, RELAXATION AND DETECTION MECHANISMS. (U)
FEB 80 C H VOLK F49620-77-C-0087
6/CSD-TR-404417 AFOSR-TR-80-0170 NL

AFOSR-TR-80-0170

NL

1994

END
DATE
FILMED
4 80
DTIC

UNCLASSIFIED

(9) Annual technical rept. Feb 79-Jan 8

SECURITY CLASSIFICATION OF THIS PAGE (When Data Entered)

19 REPORT DOCUMENTATION PAGE		READ INSTRUCTIONS BEFORE COMPLETING FORM	
1. REPORT NUMBER (18) AFOSR/TR-88-0170	2. GOVT ACCESSION NO.	3. RECIPIENT'S CATALOG NUMBER	
4. TITLE (and Subtitle) (6) NUCLEAR MOMENT ALIGNMENT, RELAXATION AND DETECTION MECHANISMS.		5. TYPE OF REPORT & PERIOD COVERED INTERIM	
7. AUTHOR(s) (10) C. H. Volk		6. PERFORMING ORG. REPORT NUMBER 404417	
(16) 53911 (17) 147		8. CONTRACT OR GRANT NUMBER(s) (15) F49628-77-C-0047	
9. PERFORMING ORGANIZATION NAME AND ADDRESS Litton, Guidance & Control Systems 5500 Canoga Ave. Woodland Hills, CA. 91365		10. PROGRAM ELEMENT, PROJECT, TASK AREA & WORK UNIT NUMBERS 61102F 2301/A4	
11. CONTROLLING OFFICE NAME AND ADDRESS Air Force Office of Scientific Research Attn: NP Building 410, Bolling AFB, D. C. 20332		12. REPORT DATE (17) February 1980	
14. MONITORING AGENCY NAME & ADDRESS (if different from Controlling Office) (14) G/CSD-TT-444417		13. NUMBER OF PAGES 62	
		15. SECURITY CLASS. (of this report) UNCLASSIFIED	
16. DISTRIBUTION STATEMENT (of this Report) Approved for public release; distribution unlimited.		15a. DECLASSIFICATION/DOWNGRADING SCHEDULE (12) 63	
17. DISTRIBUTION STATEMENT (of the abstract entered in Block 20, if different from Report)			
18. SUPPLEMENTARY NOTES			
19. KEY WORDS (Continue on reverse side if necessary and identify by block number) Nuclear Magnetic Resonance Nuclear Moment Relaxation Gyroscope Quadrupole Relaxation Optical Pumping Nuclear Moment Precession Nuclear Moment Alignment Spin Exchange			
20. ABSTRACT (Continue on reverse side if necessary and identify by block number) The reported physics research is part of an overall program to develop a nuclear magnetic resonance gyro that makes use of an optically pumped alkali metal vapor both to align the magnetic moments of the noble gas nuclei and to detect the weak magnetic fields that are generated by these precessing nuclear moments. Experimental data are described which confirm the model of the role of the alkali-atom-noble-gas-atom van der Waals molecule in the alkali-electronic-noble-gas-nuclear spin exchange interaction. Some properties of this molecule are extracted from the data together with an estimate for the spin exchange cross section in the binary alkali-atom-noble-gas-atom collisions.			

Unclassified

UNCLASSIFIED

SECURITY CLASSIFICATION OF THIS PAGE (When Data Entered)

Xe (131)

Measurements of the spin dynamic properties of Xe^{131} are described. The relaxation of Xe^{131} in the presence of an alkali vapor is attributed to spin exchange with the alkali vapor, collisions with the walls of the experimental cell, and collisions with the foreign buffer gas atoms in the cell. Estimates of the magnitudes of these relaxation contributions are made for particular experimental cells.

Unclassified

TABLE OF CONTENTS

Section		Page
I	PROGRAM DESCRIPTION.	1-1
	1.1 Introduction	1-1
	1.2 Objectives and Status of the Current Program	1-2
	1.3 Professional Personnel Associated with the Program	1-4
II	MEASUREMENT OF THE $Rb^{87}-Xe^{129}$ SPIN EXCHANGE CROSS SECTION	2-1
	2.1 Introduction	2-1
	2.2 Appendix to Section II	2-2
III	SPIN DYNAMIC EFFECTS OF Xe^{131}	3-1
	3.1 Introduction	3-1
	3.2 Appendix to Section III	3-3

Accession For	
NTIS GMA&I	<input checked="checked" type="checkbox"/>
DDC TAB	<input type="checkbox"/>
Unannounced	<input type="checkbox"/>
Justification	
By _____	
Distribution/ _____	
Availability Codes	
Dist	Avail and/or special

AIR FORCE OFFICE OF SCIENTIFIC RESEARCH (AFSC)
 NOTICE OF REVISION TO 1-12
 This report is the property of the AFSC and is
 loaned to you for use only. It is not to be
 distributed outside the AFSC. Distribution is unlimited.
 A. D. BLOSE
 Technical Information Officer

SECTION I

PROGRAM DESCRIPTION

1.1 INTRODUCTION

The Guidance and Control Systems Division of Litton Systems Inc. is involved in a multi-year program in the research and development of a nuclear magnetic resonance (NMR) gyro for use in inertial navigation systems.

In the magnetic resonance gyro, angular craft rate is sensed through a shift in the precession frequency of an ensemble of atomic or nuclear magnetic moments. The Litton NMR gyro utilizes ensembles of two noble gas isotopes in order to eliminate explicit dependence on the magnetic field. In order to obtain the gyroscopic information in this scheme, the noble gas ensembles must first be polarized so that coherent precession about an applied magnetic field can take place and, secondly, a means for detecting the nuclear precession must be provided. In the Litton approach, the noble gas ensembles attain a net magnetic moment through spin exchange with an optically oriented alkali vapor. In addition, the alkali vapor, through a magnetometer effect, detects the weak magnetic fields, which are generated by the precessing nuclear moments of the two noble gases, and thus provides the gyro angular rate information.

The purpose of the physics research program is to develop a stronger theoretical and empirical understanding of the alkali-atom-noble-gas-atom system with particular interest in the spin exchange interaction between the alkali valence electron and the noble gas nucleus, noble gas nuclear spin relaxation mechanisms as they pertain to the NMR gyro context and other related phenomena which impact the NMR gyro technology.

Results of these studies will be relevant not only to the development of an NMR gyro but also to those areas in which noble gas alkali atomic interactions are basic, as for example, the atomic frequency standard, the alkali vapor magnetometer and other such devices.

1.2 OBJECTIVES AND STATUS OF THE CURRENT PROGRAM

The research tasks described in Sections II and III of this report are part of our continuing effort to understand and parameterize the alkali-atom-noble-gas-nucleus spin exchange interaction. In addition, investigations of the spin exchange process also provide opportunities to study the pertinent relaxation mechanisms of the noble gas nuclei.

In Section II, the results of the measurements of the $\text{Rb}^{87} - \text{Xe}^{129}$ spin exchange cross section as a function of the N_2 buffer density are reported. In the last AFOSR Annual Technical Report, a theory for the

role of the alkali-atom-noble-gas-atom van der Waals molecules in the spin exchange process was developed. The theory predicts a significant dependence of the spin exchange cross section on the buffer gas density. We show that our measurements are completely consistent with this theory.

In Section III, we report on our measurements of the Rb-Xe¹³¹ spin exchange cross section and related relaxation phenomena of Xe¹³¹. Due to the nature of the Xe¹³¹ nucleus, there were problems associated with the study of the spin dynamic characteristic of Xe¹³¹ not found in the similar study of Xe¹²⁹. In order to alleviate some of these difficulties, and be able to initiate our study of the properties of Xe¹³¹, we collaborated in an experiment with a group at the University of Southern California. The advantage to us in doing this was that we could laser-pump the alkali vapor with a dye laser system, which resulted in higher alkali atomic polarizations and thus, in turn, provided larger Xe¹³¹ signals allowing us to obtain initial parameterizations of the Xe¹³¹ spin relaxation characteristics.

Investigations into this area of atomic physics have relevance not only to NMR gyro research but also to other possible areas of research such as masers, magnetometers, atomic clocks and polarized nuclear

targets. It was in this light that the results of this year's work were written up in two scientific papers: "Measurement of the $\text{Rb}^{87}\text{-Xe}^{129}$ Spin Exchange Cross Section", which was submitted to The Physical Review in consideration for publication and "Measurement of the Rb-Xe^{131} Spin Exchange Cross Section in Xe^{131} Relaxation Studies", which has been accepted for publication by Physical Review Letters. The papers are included as appendices to Sections II and III, respectively. Moreover, since these papers are a comprehensive report of our results, we provide only some necessary background statements in Sections II and III, with our findings then being contained in the appendices.

1.3 PROFESSIONAL PERSONNEL ASSOCIATED WITH THE PROGRAM

The principal investigator of these research efforts has been Dr. Charles H. Volk. This work has also been strongly supported by Dr. Tae M. Kwon, Dr. John G. Mark and Mr. Bruce C. Grover. We also wish to acknowledge the contributions of Mr. Howard E. Williams for the design and Mr. Roger L. Meyer for the construction of various components of the apparatus used in this research effort, and finally we acknowledge Dr. Edward Kanegsberg for many helpful discussions.

SECTION II
MEASUREMENT OF THE $\text{Rb}^{87}\text{-Xe}^{129}$ SPIN EXCHANGE
CROSS SECTION

2.1 INTRODUCTION

In a previous report, a theory of the role of the alkali-atom-noble-gas-atom van der Waals molecules in the alkali-electronic-noble-gas-nuclear spin exchange interaction was developed and some preliminary data supporting this theory were presented. It was noted at that time, that the agreement between the data and the model was not sufficient in order to make definitive conclusions concerning the model.

Subsequent investigations revealed that an assumption, which we had made concerning the decay of the noble gas nuclear spin, was not valid over the entire range of our measurements. In particular, it was assumed that the alkali electronic spin polarization has a zero time average in a Larmor period of the noble gas nucleus, and hence there was no dynamic polarization coupling of the alkali electron with the noble gas nucleus during the decay mode of our experiment. We found that in certain circumstances this condition was violated, resulting in a distortion of the noble gas relaxation signal and hence an erroneous estimate of the spin relaxation rate. The solution to this difficulty was to simply force the alkali polarization to zero during the greater part of the decay mode time. This was accomplished by simply blocking the detection light beam and

then letting the noble gas nuclear spin decay 'in the dark'. The detection light beam was used only to ascertain the initial and final signal amplitudes in order to determine the noble gas decay rate.

The data are found to agree with the model to within about 7 percent. We find the magnitude of this error to be an indication of the relative sophistication of the model, and further error reduction could be attained only in a more elaborate model.

2.2 APPENDIX TO SECTION II

The details of our measurements and the presentation and interpretation of our data are provided in the paper, "Measurement of the $\text{Rb}^{87}\text{-Xe}^{129}$ spin exchange cross section", by C. H. Volk, T. M. Kwon and J. G. Mark. This paper has been submitted to The Physical Review for publication.

Measurement of the $\text{Rb}^{87}\text{-Xe}^{129}$ spin
exchange cross section

C. H. Volk, T. M. Kwon, and J. G. Mark
Litton Guidance & Control Systems
5500 Canoga Ave. Woodland Hills, CA 91364

The $\text{Rb}^{87}\text{-Xe}^{129}$ spin exchange cross section has been measured in N_2 buffered cells as a function of the N_2 density using an alkali vapor magnetometer technique. The strong dependence of the spin exchange cross section on the N_2 density indicates a significant role for the Rb-Xe van der Waals molecule in the spin exchange process. Our data have allowed us to estimate the Rb-Xe molecular formation rate, which is in reasonable agreement with previous measurements. The extrapolated binary spin exchange cross section term is found to be;

$$\sigma_{\text{ex}} \bar{V}^2 = 1.5 \times 10^{-10} \text{ cm}^4 \text{ sec}^{-2}.$$

I. INTRODUCTION

The transfer of angular momentum from an electronically polarized alkali atom to an unpolarized noble gas nucleus in spin exchange collisions has been the subject of both experimental and theoretical investigations. Bouchiat, Carver, and Varnum¹ first observed the nuclear polarization of He³ used as the buffer gas for the optical pumping of natural Rb vapor. The spin exchange process was studied in more detail by Gamlin and Carver² and then subsequently by Fitzsimmons, Tankersley, and Walters³ who did a preliminary study of the effects of aluminosilicate containers on the attainable nuclear polarization. More recently Sobell⁴ considered spin exchange effects of Na with He, H₂, and D₂ in the relaxation of optically polarized Na vapor. Experimental determinations of the alkali-atom-noble-gas nuclear spin exchange cross section has been in good agreement with Herman's calculations⁵, in which he attributed the spin exchange to the contact hyperfine interaction between the noble gas nucleus and the alkali valence electron.

We report here our study of the spin exchange process between optically oriented Rb vapor and the noble gas nucleus, Xe¹²⁹, which has nuclear spin, $I = 1/2$. Some preliminary aspects of this work were previously published.⁶ We observe in our work the transverse

relaxation of Xe^{129} after it has been polarized in collisions with the oriented Rb vapor. Measurements of the relaxation rate are done as a function of both the cell temperature and the buffer gas density. From the measurements of the relaxation rate as a function of temperature, one can deduce the spin exchange cross section knowing the Rb density. The buffer gas density dependence of the cross section yields information concerning the role of the Rb-Xe van der Waals molecules in the alkali electronic noble gas nuclear spin exchange process.

II. THEORY

Herman⁵ has shown that the spin exchange mechanism between an alkali valence electron and a noble gas nucleus can be described in terms of a contact hyperfine interaction governed by the effective hamiltonian:

$$H_{\text{eff}} = \hbar \gamma \vec{I} \cdot \vec{S} \quad (1)$$

where \hbar is Plank's constant divided by 2π , γ is the strength of the interaction, \vec{I} is the spin angular momentum of the noble gas nucleus and \vec{S} is the electronic spin of the alkali atom.

If we neglect the nuclear spin of the alkali atom, then the spin exchange between the alkali atom and the Xe^{129} noble gas nucleus reduces simply to that of spin exchange between two spin 1/2 systems. Designate the expectation value of the longitudinal component of nuclear polarization of the noble gas atom as $\langle I_L \rangle$ and the expectation value of the longitudinal component of the electronic polarization of the alkali atom as, $\langle S_L \rangle$, then it can be shown that the time rate of change of the nuclear polarization due to spin exchange is given by:⁷⁻¹⁰

$$\langle \dot{I}_L \rangle = -T_{\text{ex}}^{-1} [\langle I_L \rangle - \langle S_L \rangle] \quad (2)$$

where T_{ex}^{-1} is the spin exchange rate between the noble gas nucleus and the alkali atom; which is given in terms of the interaction strength:

$$T_{\text{ex}}^{-1} = T_f^{-1/2} \frac{\langle \gamma \rangle^2 \tau_c^2}{1 + \langle \gamma \rangle^2 \tau_c^2} \quad (3)$$

where T_f^{-1} is the collision frequency, $\langle \gamma \rangle$ is an average interaction strength, and τ_c is the correlation time of the interaction. The spin exchange rate can also be written in terms of a spin exchange cross section:

$$T_{\text{ex}}^{-1} = N_A \sigma_{\text{ex}} \bar{V} \quad (4)$$

where N_A is the alkali number density, σ_{ex} is the spin exchange cross section, and \bar{V} is the alkali-atom-noble-gas-atom relative velocity. An expression for the spin exchange cross section was derived by Herman⁵:

$$\sigma_{ex} = \frac{2}{3} \left(\frac{8\pi g_n \beta_n \beta u_1 (b_o)^2 \eta (b_o)^2 b_o}{3 \hbar \bar{V}} \right) I(I+1) \sigma_{kin} \quad (5)$$

where g_n is the nuclear gyromagnetic ratio of the noble gas atom, β_n is the nuclear magneton, β is the Bohr magneton, $u_1 (b_o)^2$ is the probability density for locating the alkali valence electron at a distance equal to the internuclear separation from the alkali nucleus, $\eta (b_o)$ is the exchange enhancement factor, b_o is the kinetic radius for the collision pair, the $\sigma_{kin} = \pi b_o^2$ is the kinetic cross section.

The transverse nuclear polarization is found to obey a similar equation:

$$\langle \dot{I}^+ \rangle = T_{ex}^{-1} \left\{ \left[\langle I^+ \rangle - \langle S^+ \rangle \right] + (i \langle Y \rangle \tau_c) \left[\langle S_L \rangle \langle I^+ \rangle - \langle I_L \rangle \langle S^+ \rangle \right] \right\} \quad (6)$$

where $\langle I^+ \rangle$ ($\langle S^+ \rangle$) is the expectation value of the transverse nuclear (electronic) polarization, defined in the usual way. The imaginary term of Eq. (6) is the shift of the nuclear Zeeman energy levels due to the spin exchange interaction. Equations analogous to Eq. (2) and (6) can be written for the spin polarization of the alkali valence electron.

Since the time constants associated with the alkali electronic spin are about three orders of magnitude shorter than those associated with the noble gas nuclear spin, we can treat the alkali spin as if it were in steady state, when considering the noble gas nuclear spin dynamics. Then, in the presence of other relaxation mechanisms, the rate of change of the longitudinal noble gas nuclear spin becomes:

$$\langle \dot{I}_L \rangle = -T_{\text{ex}}^{-1} [\langle I_L \rangle - \langle S_L^0 \rangle] - T_1^{-1} \langle I_L \rangle \quad (7)$$

where $\langle S_L^0 \rangle$ denotes the steady-state value of the alkali polarization. The steady-state noble gas nuclear polarization is then found to be:

$$\langle I_L^0 \rangle = T_p / T_{\text{ex}} \langle S_L^0 \rangle \quad (8)$$

where $T_p^{-1} = T_{\text{ex}}^{-1} + T_1^{-1}$, and T_1^{-1} is the sum of all other rates contributing to the longitudinal relaxation of the noble gas nuclear spin.

Measurement of the transverse nuclear spin polarization is accomplished by causing the polarized ensembles of both the noble gas and alkali atoms to precess in a plane containing the light beam. If the time average of the alkali transverse polarization is zero in a Larmor period of the noble gas nucleus, then by Eq. (6), the time

dependence of the transverse noble gas spin polarization can be shown to have the following form:

$$\langle I^+ (t) \rangle = \langle I_L^0 \rangle \exp(-t/T_2) \sin(\Omega t + \psi) \quad (9)$$

where T_2 is the total transverse decay time, Ω is the precessional frequency of the nuclear ensemble, and ψ is the initial phase of the precessing ensemble.

III. EXPERIMENTAL

The Experimental Apparatus. The experimental apparatus is shown schematically in Figure 1. The apparatus consists of the experimental cell, which is a 15-ml Pyrex sphere. Cells are prefilled on a separate vacuum system with an excess of Rb^{87} metal, 0.5 Torr Xe^{129} , and N_2 as a buffer gas.

The cell is centered in a resistance-heated oven, provided with Pyrex windows at either end. The oven provides controlled temperatures to 80°C ($\pm 0.1^\circ\text{C}$) with a temperature uniformity across the cell of about 1°C . The oven is contained in a cylindrical coil form, providing three mutually perpendicular Helmholtz coils arranged along the x, y, and z axes. In addition correction turns along the x axis allow for the

correction of magnetic field gradients and a pair of reverse Helmholtz coils along the y and z axes provide a source of nuclear relaxation (magnetic field gradient relaxation)² in order to be able to force the nuclear magnetization to zero. The oven assembly is within four cylindrically concentric magnetic shields with the innermost shield provided with endcaps with 3-inch access holes. The magnetic shields reduce the external magnetic fields to below 10 μ G.

The light source of the optical pumping and detection is an alkali resonance lamp of the Bell, Bloom, Lynch type.¹¹ The light is passed through a D₁ filter and a circular polarizer and piped to the cell through a plastic light pipe. On the detection side, the light transmitted through the cell is piped through a plastic light pipe to a photodiode.

Polarization of the Noble Gas Nuclear Spin Ensemble. The noble gas nuclei are polarized through spin exchange collisions with the optically oriented alkali vapor. The alkali vapor is polarized by the absorption of σ^+ D₁ light in a standard longitudinal pumping scheme; this configuration is shown in Figure 2. The pumping takes place in the presence of a longitudinal magnetic field of approximately 2 mG. From

Eq. (7) and (8) one sees that the longitudinal noble gas polarization obeys the following pumping law, given the initial condition, $\langle I_L(t=0) \rangle$

$$\langle I_L(t) \rangle = \langle I_L^0 \rangle (1 - \exp(-t/T_p)) \quad (10)$$

The nuclear spins are "pumped" for a time sufficient to build up a significant polarization along the light beam direction. This time can range from 30 minutes at cell temperatures below 40°C to a few minutes at cell temperature above 70°C.

Detection of the Transverse Spin Decay of the Noble Gas Nuclei.

Measurement of the decay of the noble gas nuclear spin polarization is accomplished by switching the longitudinal pump field off and at the same time applying a precessional field along the y axis, ($\sim 100\mu\text{G}$). The fields are switched in a time short enough to guarantee that the spin systems precess about the y axis. An ac field (8 kHz) is then applied along the z axis, to utilize the alkali vapor as a magnetometer, as discussed below. The equivalent field associated with the precessing nuclear moments are detected by the magnetometer, and thus the decay characteristics of the nuclear spin systems are observed. The magnetic field arrangement for the detection mode is shown in Figure 3.

The Alkali Magnetometer. The magnetometer mechanization of the alkali vapor, which we use to detect the noble gas nuclear polarization, was first devised by Cohen-Tannoudji et al¹² and first used to detect¹³ the nuclear polarization of He³. We quote from their results as they apply to our experiment.

Consider an alkali vapor cell, as shown in Figure 4, illuminated by $\sigma^+ D_1$ light along the x axis in the presence of a static magnetic field, H_0 , and an ac magnetic field, $H_1 \cos(\omega t)$, both applied along the z axis. The intensity of the transmitted light through the cell in this configuration has been shown to be sensitive to the x component of the alkali magnetization.¹⁴ From ref. (10), we write the transverse alkali polarization as:

$$\frac{M^+}{M'_0} = A_0 + \sum_{p=1}^{\infty} (A_p \exp(ip\omega t) + A_{-p} \exp(-ip\omega t)) \quad (11)$$

where M'_0 is defined by the steady-state alkali magnetization in the presence of relaxation and

$$A_0 = \sum_{n=-\infty}^{\infty} \frac{J_n^2(\omega_1/\omega)}{1 + i(\omega_0 + n\omega)\tau} \quad (12a)$$

and

$$A_p = \sum_{n=-\infty}^{\infty} \frac{J_n(\omega_1/\omega) J_{n+p}(\omega_1/\omega)}{1 + i(\omega_0 + n\omega)\tau} \quad (12b)$$

where $\omega_0 = H_0 \gamma_A$, $\omega_1 = H_1 \gamma_A$ with γ_A the gyromagnetic ratio of the alkali valence electron, τ is the spin relaxation time of the alkali vapor, and $J_n(\omega_1/\omega)$ is a Bessel function of order n when $n \geq 0$. For $n < 0$, one has:

$$J_n(\omega_1/\omega) = (-1)^n J_{-n}(\omega_1/\omega) \quad (13)$$

Since $M_x = \text{Re} [M^+]$ we can deduce the behavior of M_x and hence the optical signal from Eq. (11), (12), and (12b). One sees then that M_x is a periodic function in time with period $2\pi/\omega$, and the light transmitted through the cell is modulated at various harmonics p of ω which depends on A_p and A_{-p} given in Eq. (12b). In addition one can see that the signal undergoes a resonance when the field is swept about the values for which $(\omega_0 + n\omega) = 0$. Thus at each modulation, p resonates from $\omega_0 = 0$, $\omega_0 = \pm\omega$, The width of these resonances is independent of n and is $\Delta\omega_0 = 2/\tau$. The amplitude of the resonance of order n , detected at the harmonic p , is given by the Bessel function $J_n(\omega_1/\omega) J_{n \pm p}(\omega_1/\omega)$.

In our experiment we operate at the $n = 0$ resonance and detect the $p = 1$ modulation. For the case of a constant magnetic field along the z axis the signal is found to have the following proportionality:

$$S \propto M'_0 J_0(\omega_1/\omega) J_1(\omega_1/\omega) \frac{\omega_0}{1+(\omega_0\tau)^2} \sin(\omega t) \quad (14)$$

for $\omega_0 \ll 1$, the signal is seen to be proportional to the field along the z axis in first order.

In our experimental arrangement, because of the presence of the y axis precessional field and because of the rotation of the nuclear field in the x, z plane, there are fields along all three axes. The expression for the signal in the $n = 0$, $p = 1$ mode for the case of a general magnetic field is given by¹⁵:

$$S \propto M'_0 / \Gamma J_0(\omega_1/\omega) J_1(\omega_1/\omega) \frac{\Gamma \bar{\omega}_z + \bar{\omega}_x \bar{\omega}_y}{\Gamma^2 + \bar{\omega}_x^2 + \bar{\omega}_y^2 + \bar{\omega}_z^2} \sin(\omega t) \quad (15)$$

where $\Gamma = 1/\tau$, $\bar{\omega}_z = \omega_z$, and $\bar{\omega}_{y,x} = J_0(\omega_1/\omega) \omega_{y,x} = J_0(\omega_1/\omega) \gamma_A H_{y,x}$

with

$$\omega_z = \gamma_A H_e^{NG} \cos(\Omega t) \quad (16a)$$

$$\omega_x = \gamma_A H_e^{NG} \sin(\Omega t) \quad (16b)$$

where H_e^{NG} is the magnitude of the equivalent magnetic field due to the noble gas nuclei, as seen by the alkali atoms. Since $\Omega \ll \omega$, we

take the nuclear field as approximately dc and substitute the expressions given in Eq. (16a) and (16b) directly into Eq. (15), using the condition, $\Gamma \gg \omega_x, \omega_z$. Then one finds:

$$M_o' J_o(\omega_1/\omega) J_1(\omega_1/\omega) \gamma_A H_e^{NG} \frac{\sqrt{\Gamma^2 + J_o^4(\omega_1/\omega) \gamma_A^2 H_y^2}}{\Gamma^2 + J_o^2(\omega_1/\omega) \gamma_A^2 H_y^2} \cos(\Omega t + \psi) \sin(\omega t) \quad (17)$$

The signal then is seen to be proportional to the magnitude of the nuclear field, doubly modulated at the frequency, ω , and the nuclear precession frequency, Ω .

The Experimental Procedure. A measurement of the noble gas transverse decay rate is made in the following manner. An experimental cell is situated in the apparatus. The fields present at the cell are balanced to zero with the Helmholtz coils on each axis by employing the results of the signal expression in Eq. (15). At first all fields are close to zero with no compensation due to the magnetic shielding. Next a low-frequency (10-Hz) external sinusoidal field is applied along either the x or y axes; the induced signal can then be minimized by forcing the field along the y or x directions, respectively, to zero by applying a compensating field with the appropriate Helmholtz coil. The z axis can be compensated by applying a dc field that forces the dc

component of the induced signal to zero. The signal sensitivity is then maximized by applying the external field along the z axis and then adjusting the ac amplitude, ω_1 , to maximize the Bessel function product, $J_0(\omega_1/\omega)J_1(\omega_1/\omega)$. A longitudinal noble gas polarization can now be attained by applying a dc field along the direction of the light beam.

In our experimental measurements the detection light is blocked, for the most part, during the decay of the nuclear spin. The cell is illuminated for about a noble gas Larmor period at the beginning of the decay and again some time later. The noble gas relaxation time, T_2 , is deduced from Eq. (9) knowing the signal strengths at the times when the cell is illuminated and the time the spin decaying in the "dark". This procedure insures that the transverse alkali spin is zero and hence decoupled from the noble gas spin decay.

IV. RESULTS

The total transverse decay rate, $1/T_2$, defined in Eq. (9), is assumed to be of the form:

$$\begin{aligned} T_2^{-1} &= T_{\text{ex}}^{-1} + (T'_2)^{-1} \\ &= N_{\text{Rb}} \sigma_{\text{ex}} \bar{V} + (T'_2)^{-1} \end{aligned} \quad (18)$$

where to first order, the variation of T_2 to temperature is due to spin exchange. Observing from Eq. (5) that the spin exchange cross section is inversely proportional to the relative velocity squared, we plot in Figure 5 typical relaxation rate data versus the term, N_{Rb}/\bar{V} . We have taken the Rb number density to be given by the saturated formula¹⁶:

$$\log(N_{\text{Rb}}) = -4560/T + 30.98 - 2.45\log(T) \quad (19)$$

where T is the cell temperature in Kelvin. We perform a linear least-squares fit to the data such as that represented in Figure 5. The estimate of the slope corresponds to the temperature-independent exchange term, $\sigma \bar{V}^2$, and the intercept represents the sum of all other relaxation rates, $1/T'_2$, which in the case of Xe^{129} is mostly due to magnetic field gradient relaxation. Finally, in Figure 6, we plot the measured spin exchange cross section versus N_2 buffer density in the cell.

The Role of Molecular Formation in the Spin Exchange Process. We believe that the results displayed in Figure 6 are an indication of a role of the Rb-Xe diatomic molecule in the spin exchange process. The solid line curve in Figure 6 represents a least-squares fit of the data to a simplistic molecular model of the exchange process.

We take the exchange rate between the Rb electronic spin and the Xe nuclear spin to have contributions from bound molecular type collisions and binary type collisions, which are independent, and hence we can write the total exchange rate at:

$$T_{\text{ex}}^{-1} = T_{\text{ex(molecule)}}^{-1} + T_{\text{ex(binary)}}^{-1} \quad (20)$$

where both contributions can be written in terms of a spin exchange cross section as in Eq. (4). We neglect the effects of quasi-bound molecules following the results of a previous study of the Rb-Xe molecule.¹⁷ For bound molecules, which are formed in 3-body collisions, we take the third body to be an N_2 molecule, which is always by far in greatest abundance. In this case then, we have that the molecular formation rate is proportional to the density of N_2 . Taking the correlation time of the interaction to be the duration of the collision, then τ_c is inversely proportional to the density of N_2 , since the Rb-Xe molecule exists only until it experiences a collision. Again, because of the relative number densities in this work, we take the breakup body

always to be an N_2 molecule. The short binary collisions between the Rb and Xe atoms are independent of the N_2 density. As a function of N_2 density we can rewrite Eq. (20) as:

$$T_{\text{ex}}^{-1} = (a\rho)^{1/2} \frac{(b/\rho^2)}{1+(b/\rho^2)} + c \quad (21)$$

Rearranging the terms we find:

$$T_{\text{ex}}^{-1} = 1/2 \frac{ab\rho}{b+\rho^2} + c \quad (22)$$

where ρ is the density of N_2 ; the factor, a , corresponds to the molecular formation rate; b represents the average interaction strength correlation time product; and c is simply the binary exchange rate.

Evaluation of the Parameters. A least-squares fit of our data to the functional form of Eq. (22) yielded the following information:

1. The three body collision rate of Rb, Xe, and N_2 per Xe atom was found to be:

$$T_f^{-1} = 4.5 \pm 0.5 \times 10^{-4} \text{ sec}^{-1} / \text{Torr } N_2 \quad (23)$$

when evaluated at 273K. Bouchiat et al¹⁸ evaluated the formation rate of Rb-Xe molecules in the presence of Xe only. Normalizing our formation rate per Torr Xe and converting to a formation

rate per Rb atom, we find that our value differs from the one reported by Bouchiat by about 12%. The significance of this comparison lies only in the order of magnitude agreement, since the work of Bouchiat et al was concerned with a different three body collision.

2. The average strength of the interaction multiplied by the duration of the collision per Torr N_2 was found to be:

$$\langle \gamma \rangle \tau_c \sim 15 \quad (24)$$

If we assume that the lifetime of the molecule is limited by N_2 collisions, we can use standard gas kinetic arguments to estimate:

$$\tau_c = 0.5 \times 10^{-7} \text{ sec/Torr } N_2 \quad (25)$$

Substituting this value into Eq. (24), we find the average interaction strength:

$$\langle \gamma \rangle \sim 3 \times 10^8 \text{ sec}^{-1} \quad (26)$$

This value is only of order of magnitude agreement with that estimated previously for the binary collisions,^{7,8} but that seems to be reasonable agreement considering the approximations used in the theory.

3. The binary spin exchange term was found to be:

$$\sigma_{\text{ex}} \nabla = 1.5 \pm 0.2 \times 10^{-10} \text{ cm}^4 \text{ sec}^{-2} \quad (27)$$

A previous measurement of the exchange cross section for $\text{Rb}^{87}\text{-Xe}^{129}$ was made by Grover⁶ in cells buffered with 500 Torr He^4 . Extrapolating our values for N_2 out of 500 Torr, we find a difference of about 30% between our value and Grover's. The difference may lie in either different molecular kinematics for He-buffered cells or in the fact that Grover's relaxation measurements were not done in the "dark", which would possibly have resulted in a distortion of the Xe relaxation signal.

Evaluating the spin exchange cross section at 65C, we find:
 $\sigma_{\text{ex}} = 1.1 \times 10^{-19} \text{ cm}^2$. This value is about four times larger than what had been theoretically estimated using the Herman-Skillman wavefunction tabulations.⁸ We think that this is reasonable agreement considering the uncertainty in the parameters that enter into the calculations. For instance the entire factor of four could result from only a 20% error in the Rb wavefunction because this parameter enters twice, each time raised to the fourth power.

V. SUMMARY

The measurement of the $\text{Rb}^{87} - \text{Xe}^{129}$ spin exchange cross section has indicated a significant role of the Rb-Xe van der Waals molecule in the spin exchange process. Our estimate of the molecular formation rate for the Rb-Xe molecule is in reasonable agreement with the previously measured formation rate,¹⁸ which we take to be supportive of our model of molecular-enhanced spin exchange. Although our estimate of the Rb-Xe spin exchange cross section is much larger than theoretical estimates, we think that the overall agreement is generally good, and discrepancies are indicative of the uncertainties in the theory.

Since there has been recent evidence for the existence of alkali-atom-noble-gas-atom van der Waals molecules with light noble gases,¹⁹ one might expect a similar molecular-enhanced spin exchange cross section for He^3 and Ne^{21} , which may be of interest in the consideration of polarized nuclear targets.

The attainable nuclear polarization is seen from Eq. (8) to depend on the T_1 relaxation of the nuclear ensemble and the saturated value of the alkali polarization. In our study of Xe^{129} , the dominant source of T_1 relaxation was due to magnetic field inhomogeneities. Achieving nuclear

polarizations better than 90% of the alkali polarization in our present apparatus would imply cell temperatures of greater than only 60C, for a sample buffered with between 15 and 25 Torr N_2 . We note that the field inhomogenities could have been further reduced from what we tolerated in our experiment through the use of higher order corrections on the magnetic field. This would have in effect lowered the already moderate cell temperature at which one could attain relatively high nuclear polarizations. Alkali ground state polarizations approaching 100%, through the use of laser pumping, have recently been reported²⁰ in samples of Na with densities of 10^{12} cm^{-3} . This alkali density is an order of magnitude larger than the Rb densities in our experiment. It is then quite feasible to expect nuclear polarizations approaching 100% in controlled environments through exchange with a laser-pumped alkali vapor ensemble.

VI. ACKNOWLEDGMENT

We would like to acknowledge the contributions of Dr. E. Kanegsberg in the area of observing alkali-atom-noble-gas-nucleus spin exchange using the magnetometer technique and for his helpful comments in the preparation of this paper. We are also thankful for the talents of Mr. R. L. Meyer and Mr. H. E. Williams for their design and construction of the apparatus used in this work. This research was partially supported under an Air Force Office of Scientific Research contract No. F49620-77-C-0047.

REFERENCES

1. M.A. Bouchiat, T.R. Carver and C.M. Varnum, Phys. Rev. Lett. 5, 373 (1960).
2. R.L. Gamblin and T.R. Carver, Phys. Rev. 138A, 946 (1965)
3. W.A. Fitzsimmons, L.L. Tankersley and G.K. Walters, Phys. Rev. 179, 156 (1969).
4. H. Sobell, Z. Natur. 24, 2023 (1969); Phys. Lett. 41A, 373 (1972); Z. Phys. 265, 487 (1973).
5. R.M. Herman, Phys. Rev. 137A, 1062 (1965).
6. B.C. Grover, Phys. Rev. Lett. 40, 391 (1978).
7. F.G. Major, Litton Subcontract Report, No. WC376807, (unpublished).
8. C.H. Volk, B.C. Grover, and E. Kanegsberg, AFOSR, Annual Technical Report (1978) (unpublished).
9. H.G. Dehmelt, Phys. Rev. 109, 381 (1958).
10. L.C. Balling, R.J. Hanson and F.M. Pipkin, Phys. Rev. 133, A607 (1964).
11. W.E. Bell, A.L. Bloom and J. Lynch, Rev. Sci. Instru. 32, 688 (1961).
12. C. Cohen-Tannoudji, J. Dupont-Roc, S. Haroch, and F. Laloe, Rev. de Phys. Appl. 5, 102 (1970).

13. C. Cohen-Tannoudji, J. Dupond-Roc, S. Haroch, and F. Laloe, Phys. Rev. Lett. 22, 758 (1969).
14. M.A. Bouchiat, J. de Phys. 26, 415 (1965).
15. J. Dupont-Roc, Rev. de Phys. Appl. 5, 853 (1970).
16. C.J. Smithells, Metals Reference Book, Vol. 2 (Butterworths London, 1962), p. 655.
17. C.C. Bouchiat, M.A. Bouchiat, L.C.L Pottier, Phys. Rev. 181, 3144 (1969).
18. M.A. Bouchiat, J. Brossel and L.C. Pottier, J. Chem Phys. 56, 3703 (1972).
19. F.A. Franz and C.H. Volk, phys. Rev. Lett. 35, 1704 (1975); Phys. Rev. 14A, 1711 (1976); 18A, 599 (1978).
20. A.C. Tam and W. Happer, Appl. Phys. Lett. 30, 580 (1977).

FIGURE CAPTIONS

Figure 1. Schematic representation of the experimental apparatus.

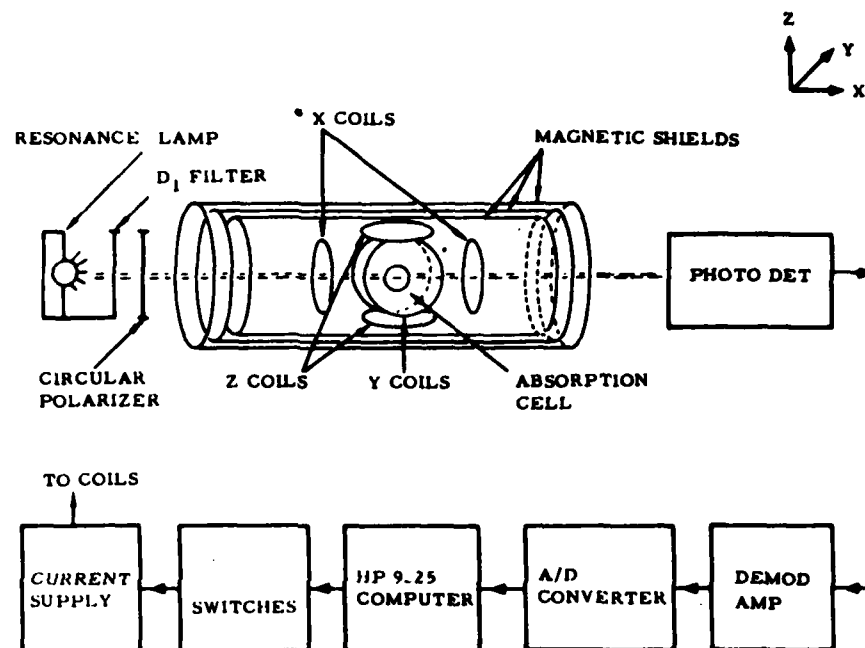
Figure 2. Magnetic field arrangement for the longitudinal pumping of the alkali vapor.

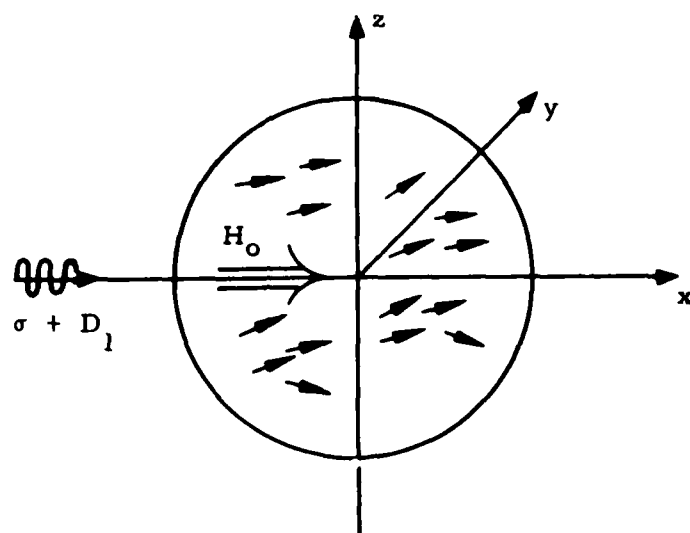
Figure 3. Magnetic field arrangement for the detection of the noble gas nuclear spins.

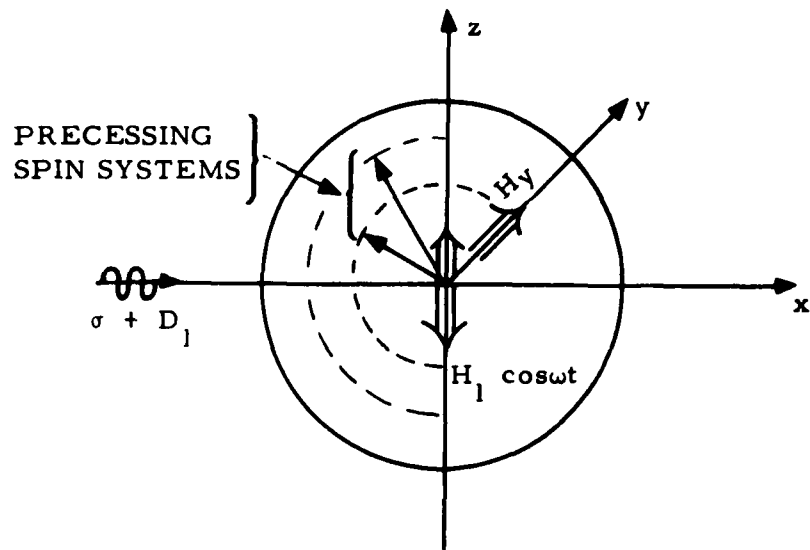
Figure 4. Magnetic field arrangement for the magnetometer mechanization of the alkali vapor.

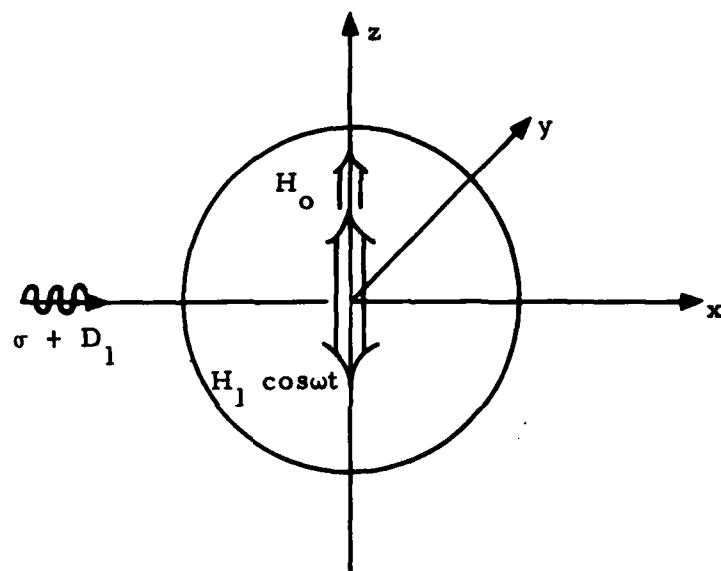
Figure 5. Typical plot of the Xe relaxation rate versus $N_{\text{Rb}} \bar{V}$. The solid line represents a linear least-squares fit of the experimental data, where the slope of the line represents the spin exchange cross section term, and the intercept is the sum of all other relaxation rates. The error bars on the data points are a standard deviation of repeated trials. These data were taken from a cell containing Rb^{87} , 0.5 Torr Xe^{129} and 74.5 Torr N_2 . The least-squares fit yielded a temperature independent rate of $3.67 \pm 0.3 \times 10^{-4} \text{ sec}^{-1}$ and $\sigma_{\text{ex}} \bar{V}^2 = 4.07 \pm 0.35 \times 10^{-10} \text{ cm}^4 \text{ sec}^{-2}$.

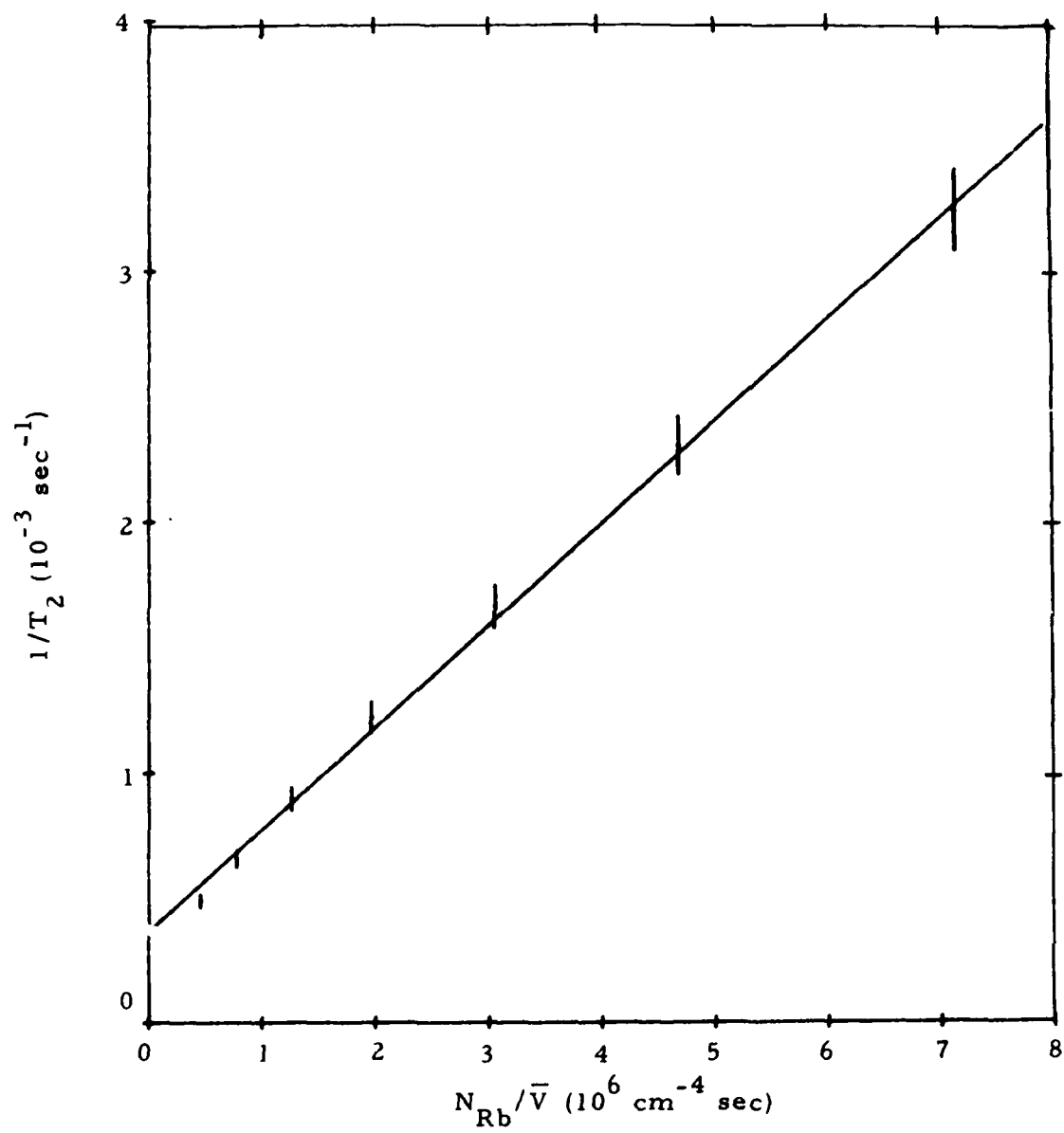
Figure 6. Plot of the spin exchange cross section term versus the N_2 pressure. The solid line is least-squares fit of the data to our molecular spin exchange model. The error bars on the data points represent a standard deviation for repeated trials.

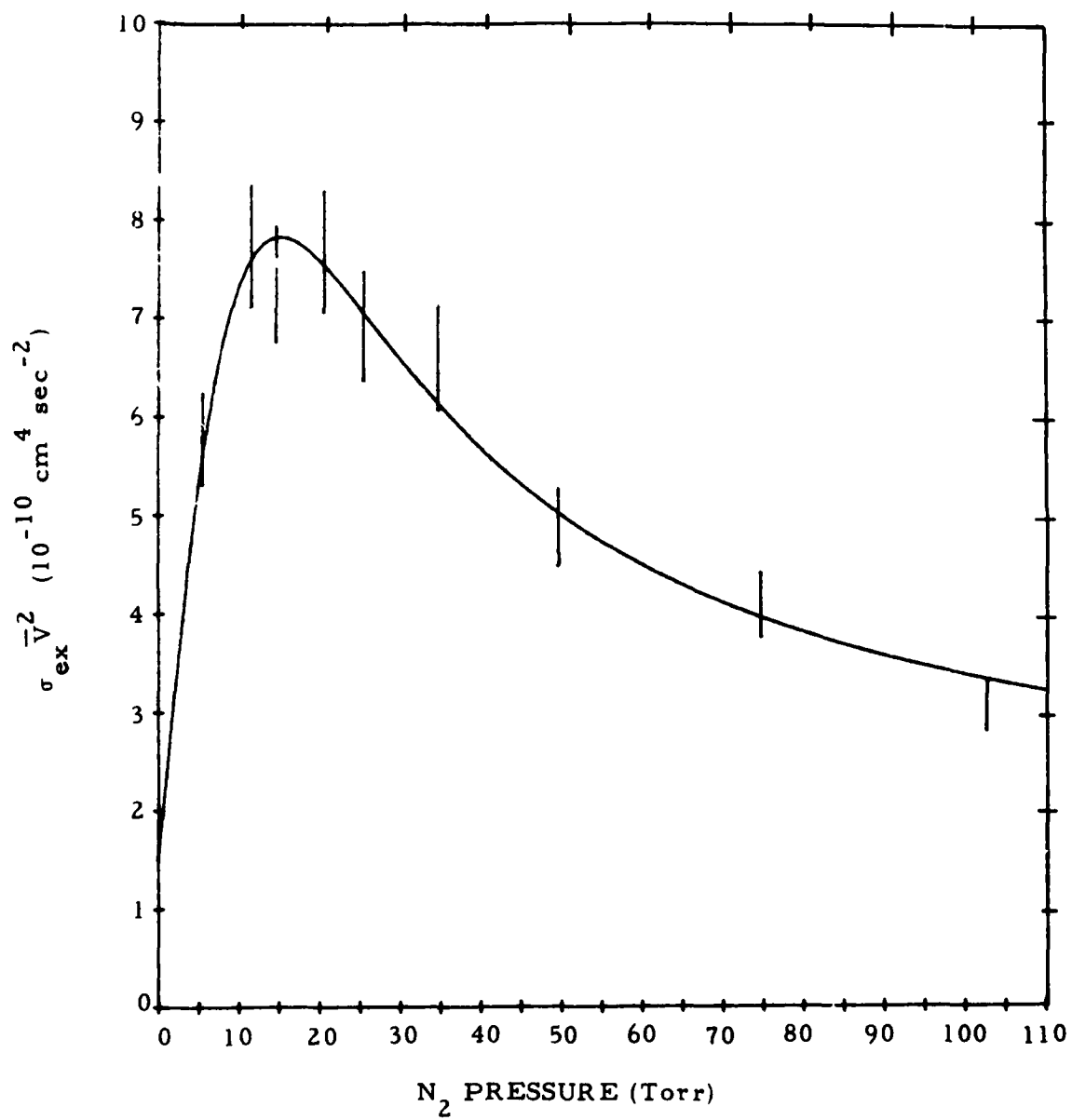












SECTION III

SPIN DYNAMIC EFFECTS OF Xe^{131}

3.1 INTRODUCTION

The noble gas nucleus, Xe^{131} , exhibits significantly different spin dynamic characteristics, as compared to Xe^{129} , primarily due to the fact that it has nuclear spin $I = 3/2$, and thus possesses a nuclear electric quadrupole moment and hence additional interaction channels. The nuclear electric quadrupole moment interacts with electric field gradients present at the nucleus and this results in spin relaxation through transitions between the Zeeman levels and inhomogeneous broadening of those levels. A possible origin of the electric field gradients of sufficient magnitude to cause nuclear spin relaxation is the deformation of the noble gas electronic shells which occurs in collisions of the noble gas atom with the walls of the cell and in collisions with other atoms in the cell. In this case then, one would expect the Xe^{131} to exhibit a relaxation rate dependent on the cell walls and on the buffer gas atoms in the cell. These are effects not observed in the relaxation of Xe^{129} . These relaxation modes in the case of Xe^{131} are clearly demonstrated by our data. We have used a model to analyze the data in which the relaxation is attributed to

- a) spin exchange with the alkali vapor,
- b) collisions with the cell walls,
- and c) a constant rate which we attribute to gas phase collisions.

Agreement with this model has been very good, with uncertainties in the order of 10 percent.

There are two main difficulties involved in making measurements of the spin relaxation characteristic of Xe^{131} . The relative signal amplitude is small due to the fact that the spin exchange cross section between Rb and Xe^{131} is small, experimentally determined to be about an order of magnitude smaller than that for Rb and Xe^{129} , and that the relaxation rates, primarily through the quadrupolar interaction, are much larger than those found for Xe^{129} . The second but related problem is the relatively short relaxation time, which we have found to range from about 10 to 100 seconds, resulting in an additional difficulty in the analysis of the Xe^{131} relaxation signal.

A means for overcoming at least the problem of the small signal amplitude in Xe^{131} is to increase the alkali polarization, which allows the noble gas nuclear spin to draw from a larger angular momentum reservoir. We accomplished this by laser-pumping the sample cells with a dye laser system tuned to the Rb D_1 resonance line. In this way we were able to increase the alkali polarization in addition to maintaining significant alkali polarization over a wider temperature range. The necessity of Xe^{131} data over a wide temperature range, as compared to that needed for Xe^{129} , is due to the functional form of the model.

3.2 APPENDIX TO SECTION III

The details of our work on the spin relaxation of Xe^{131} are provided in the paper, "Measurement of the Rb- Xe^{131} Spin Exchange Cross Section in Xe^{131} Relaxation Studies", by C. H. Volk, T. M. Kwon and J. G. Mark of Litton Guidance and Control Systems in collaboration with Y. B. Kim and J. C. Woo of the Department of Physics at the University of Southern California. This paper has been accepted for publication by Physical Review Letters.

Measurement of the Rb-Xe¹³¹ Spin Exchange Cross

Section in Xe¹³¹ Relaxation Studies

C. H. Volk, T. M. Kwon and J. G. Mark

Litton Guidance & Control Systems

5500 Canoga Avenue, Woodland Hills CA 91364

and

Y. B. Kim and J. C. Woo*

Department of Physics

University of Southern California

Los Angeles CA 90007

ABSTRACT

Estimates of the Rb-Xe¹³¹ spin exchange cross section have been obtained by observing the nuclear spin relaxation of Xe¹³¹ in the presence of a Rb vapor. Nuclear spin relaxation of Xe¹³¹ due to the presence of a foreign buffer gas and the relaxation rate on the glass walls of the cell have also been observed.

*SNU-AID Visiting Professor, permanent address: Department of Physics, Seoul National University, Seoul 151, Korea.

The spin exchange process between the polarized valence electron of an alkali atom and the unpolarized nucleus of a noble gas atom¹, has been of interest in the past both as a mechanism for polarizing noble gas nuclei²⁻⁵ and also as a source of relaxation for optically oriented alkali vapors.⁶ We have recently measured the transverse nuclear spin relaxation of a gaseous Xe^{131} ensemble which had been polarized in collisions with an optically oriented Rb vapor. These measurements allowed for the first time the experimental determination of the spin exchange cross section between the Rb valence electron and the nucleus of Xe^{131} . In addition, we have, to our knowledge, the first measurements of the nuclear spin relaxation rates of Xe^{131} both on the glass walls of the experimental cell and in collisions with a foreign buffer gas in a low magnetic field. Similar measurements have been previously made for He^3 in the presence of Rb^{2-4} and Na^6 and for Xe^{129} in the presence of Rb^5 .

Previous measurements of the nuclear spin relaxation of Xe^{131} , which were done in pure xenon at high pressures, showed a relaxation time that was inversely proportional to the density of the gas.⁷ The observed relaxation was attributed to a nuclear quadrupole interaction which is present during the collision of the xenon atoms. A theoretical study of this problem by Adrian⁸ confirmed that the quadrupole

interaction was the dominant relaxation mechanism of Xe^{131} in these samples. However an extrapolation of Adrian's results to our sample densities⁹ led us to expect relaxation times due to xenon-buffer-gas collisions of almost an order of magnitude longer than what we actually observed. The polarization of Xe^{131} through exchange with Rb then proved to be a more difficult problem than that associated with the other noble gas nuclei.

Our experimental setup consists of a 15 ml Pyrex sphere into which we distill an excess of Rb metal, and then fill with 0.5 Torr enriched Xe^{131} plus a buffer gas. The Xe gas is such that Xe^{131} constitutes 63.89 mole %, Xe^{129} is 0.7 mole %, Kr^{83} is 0.38 mole % and the remaining is composed of even isotopes of Xe. The buffer gases used in this particular set of measurements were H_2 , N_2 , and He^4 . The cell is contained in a resistance-heated oven capable of controlling temperatures to $\pm 0.1^\circ\text{C}$ up to 120°C . A three-axis set of Helmholtz coils surrounds the oven with the whole assembly contained in four cylindrically concentric magnetic shields, which reduce external magnetic fields to below $10\mu\text{G}$. A schematic representation of the apparatus is displayed in Figure 1.

The experiment proceeds in two steps. In the first step, the Rb vapor is optically pumped in the longitudinal direction with $\sigma^+ D_1$ light provided by a dye laser. In this mode only a single magnetic field along the light beam direction is present in order to provide a quantization axis for the Rb electronic spin and the Xe nuclear spin. With reference to Figure 1, then, in the "pump" mode, the resonance lamp is moved off axis to allow the laser beam to pump the alkali vapor. Both the resonance lamp and the D_1 filter are moved off axis when pumping.

The dye laser is a Spectra Physics model 375 with Oxazine-750 dye pumped by a Spectra Physics model 171 krypton-ion laser. The dye laser is employed because of the low polarization levels generated by pumping with the resonance lamp. The resonance lamp, although sufficient for similar measurements⁵ in Xe^{129} , could not provide Xe^{131} signal at the high temperature end. During the experiment, measurements of the laser power in front of the circularly polarizer indicated power between 80 and 150 mw. There was no concern to keep the laser power stable as long as it remained above 80 mw. The laser wavelength was centered at 7947.6 Å with a full width at half maximum of about 1 Å.

The system was pumped for a time long enough to build up a significant Xe nuclear polarization. Neglecting the nuclear spin of the alkali, the noble gas polarization can be expressed in terms of the equilibrium Rb polarization as:⁴

$$P_{\text{Xe}} = T_p P_{\text{Rb}} / T_{\text{ex}} \quad (1)$$

where $T_{\text{ex}} = (N_{\text{Rb}} \sigma_{\text{ex}} \bar{V})^{-1}$, with N_{Rb} the Rb number density, σ_{ex} the Xe-Rb spin exchange cross section and \bar{V} the Xe-Rb relative velocity. T_p is the time characteristic of the growth of the Xe nuclear polarization, which is given by:

$$T_p^{-1} = T_{\text{ex}}^{-1} + T_1^{-1} \quad (2)$$

with T_1 the longitudinal nuclear relaxation time. Pump times for the Xe in this experiment were on the order of minutes.

The second step in the experiment is to mechanize the Rb vapor as a magnetometer to detect the Xe magnetization as it precesses about the y-axis. This is accomplished by switching off the x-axis pump field and switching on an 8-kHz drive field along the z-axis and a 100 μ G precessional field along the y-axis. In this detection mode,

the resonance lamp is moved on axis to be used at the source of the detection beam, since it is a very low noise source of D_1 light. The magnetometer mechanization, which was developed by Cohen-Tannoudji et al.¹⁰, has been previously discussed in terms of measuring noble gas nuclear spin decay rates.⁵ It can be shown that in this mode the transmitted light beam is modulated at the drive frequency and at the noble gas nuclear precession frequency with a modulation amplitude proportional to the Xe magnetization.

The decay of the Xe magnetization is characterized by a time constant, T_2 , which we assume can be written in the following form:

$$T_2^{-1} = N_{\text{Rb}} \sigma_{\text{ex}} \bar{V} + \Gamma e^{2E/kT} + (T_2')^{-1} \quad (3)$$

where the first term on the RHS of Eq. (3) represents the spin exchange rate with the Rb vapor, the second term is a wall relaxation rate⁴ with Γ the effective collision rate, E the adhesion energy of the Xe atoms on the glass wall, k is Boltzmann's constant and T is the cell temperature in degrees/Kelvin, and the third term represents all other relaxation rates, which we assume are at most weakly temperature dependent.

The results of our measurements of the Xe^{131} nuclear spin decay rate as a function of cell temperature are shown in Figures 2a through d, where the solid line in each plot represents a least-squares fit of the data to the functional form of Eq. (3). Error bars represent a standard deviation based on reproduced measurements at selected temperature points. Evaluations of the relaxation parameters are given in Table I.

With reference to Table I, we make the following comments about our findings:

1. Recently extensive measurements of the Rb-Xe^{129} spin exchange cross section, in the presence of N_2 as a buffer gas, have been made.¹¹ Referring to Table I, the cross section for the Rb-Xe^{131} exchange in the presence of 20.5 Torr N_2 is a factor of sixteen smaller than the cross section for Rb-Xe^{129} in a similarly buffered cell. Using Herman's¹ expression for the spin exchange cross section, one would expect cross section values for Xe^{131} to be about half those for the corresponding Xe^{129} cases. We think that this discrepancy may be due to an additional Rb-Xe interaction, of a quadrupolar type, which lessens the efficiency

of the exchange process and hence lowers the measured cross section for Xe^{131} .

2. The variation of the Rb-Xe^{131} cross sections with buffer gas pressure, see Table I, is expected in light of the influence of the Rb-Xe diatomic molecule on the spin exchange interaction which has been established.^{11, 12} However, considering the comment in the previous paragraph, we do not expect the Xe^{131} cross section to have the same functional dependence on the buffer gas pressure as was found for Xe^{129} , see Refs. 11 and 12.

3. Since all the measurements were done in the same type cell, it is hard to say anything about the parameter, Γ , except that it is physically reasonable. The absorption energy, E , is of the right order of magnitude for the adhesion of Xe onto Pyrex.¹³

A similar wall interaction has been observed in measurements of the relaxation of Hg^{201} in quartz cells.¹⁴⁻¹⁶ The adhesion energy of Hg onto quartz derived from these measurements is

found to vary by about a factor of two; E is given at 0.18 eV in Ref. 14 and as 0.34 eV in Ref. 16. The difference in these measurements was attributed to a dependence of the Hg relaxation on the cell fabrication technique and cell temperature history. We observed no dependence of the cell temperature history on the relaxation of Xe^{131} . We are not sure whether this is due to the nature of the noble gas relaxation or the nature of the cell material.

4. The large difference between the constant rate, $1/T'_{2'}$, measured in the H_2 cell as compared to that found in the N_2 cell, we attribute to a relaxation mechanism of the Xe^{131} in collisions with the buffer gas. This type of an effect has not been observed for Xe^{129} in similar cells, and thus we believe this interaction to be of a quadrupolar type. The lack of variation of the constant rate in the He-buffered cells may be due to the insensitivity of the He data to the least squares fit.

We wish to thank R. L. Meyer, H. E. Williams, and L. McGann for the design and construction of many of the pieces of the apparatus

used in this work. This research was supported in part by the Air
Force Office of Scientific Research under Contract F49620-77-C-0047.

TABLE I
LEAST-SQUARES FIT ESTIMATES OF THE Xe^{131} RELAXATION
PARAMETERS IN DIFFERENTLY BUFFERED CELLS

Buffer Gas	$\sigma_{\text{ex}} \bar{V}^2$	Γ	E	$1/T_2$
Torr	$10^{-11}(\text{cm}^4 \text{sec}^{-2})$	10^{-8}sec^{-1}	eV	10^{-3}sec^{-1}
105 H_2	5.96 ± 0.4	3.89 ± 0.2	0.13 ± 0.01	1.54 ± 0.5
20.5 N_2	4.27 ± 0.1	0.40 ± 0.02	0.16 ± 0.01	12.5 ± 0.5
20 He	6.06 ± 1	1.47 ± 0.5	0.13 ± 0.01	7.42 ± 1
100 He	1.3 ± 2	2.85 ± 0.5	0.12 ± 0.01	7.47 ± 1

The 105 Torr H_2 cell contained Rb^{87} , and the other three cells had natural Rb. All cells contained 0.5 Torr-enriched Xe^{131} .

References

1. R.M. Herman, Phys. Rev. 137A, 1062 (1965).
2. M.A. Bouchiat, T.R. Carver and C.M. Venum, Phys. Rev. Lett. 5, 373 (1960).
3. R.L. Gamblin and T.R. Carver, Phys. Rev. 138A, 946 (1965).
4. W.A. Fitzsimmons, L.L. Tankersley and G.K. Walters, Phys. Rev. 179, 156 (1969).
5. B.C. Grover, Phys. Rev. Lett. 40, 391 (1978).
6. H. Sobell, Z. Natur. 24, 2023 (1969); Phys. Lett. 41A, 373 (1972); Z. Phys. 265, 487 (1973).
7. D. Brinkmann, E. Brun and H.H. Staub, Helv. Phys. Acta. 35, 431 (1962).
8. F.J. Adrian, Phys. Rev. 403A, (1965).
9. C.H. Volk, B.C. Grover and E. Kanegsberg, AFOSR, Annual Technical Report, Contract No. F49620-77-C-0047 (1978) (unpublished).
10. C. Cohen-Tannoudji, J. Dupont-Roc, S. Haroche and F. Laloe, Rev. Phys. Appl. 5, 95 (1970); 5, 102 (1970).
11. C.H. Volk, T.M. Kwon, B.C. Grover and J.G. Mark, "Measurement of the Rb^{87} - Xe^{129} spin exchange cross section", (in preparation).

12. C.H. Volk, AFOSR, Annual Technical Report, Contract No. F49620-77-C-0047 (1979) (unpublished).
13. B.G. Baker, L.A. Bruce and P.G. Fox, Trans. Faraday Soc. 64, 477 (1968).
14. B. Cognac and G. Lemeignan, Compt. Rend. 264, 1850 (1967).
15. I.E. Grinko, V.F. Terzeman, Yu.M. Petukhov and I.A. Shushpanov, Opt. Spectrosc. 29, 329 (1970).
16. V.P. Putyrskii and T.G. Izyumova, Opt. Spectrosc. 37, 227 (1974).

Figure Captions

Figure 1. Schematic representation of the experimental apparatus.

Figure 2. Xe^{131} relaxation rate versus cell temperature in the presence of (a) Rb^{87} and 105 Torr H_2 , (b) natural Rb and 20.5 Torr N_2 , (c) natural Rb and 20 Torr He^4 , and (d) natural Rb and 100 Torr He^4 .

